FISHERIES RESEARCH BOARD OF CANADA

MANUSCRIPT REPORTS OF THE BIOLOGICAL STATIONS

No.

514

Title

Interim Report

Mechanical Alterations to Alberni Harbour Model

Author

R. A. Pollard

1953

PACIFIC OCEANOGRAPHIC GROUP

Nanaimo, B.C.

Interim Report

MECHANICAL ALTERATIONS TO ALBERNI HARBOUR MODEL

by

R.A. Pollard

File N 7-22
February 1, 1953

FOREWORD

Von Arx (7, pp. 24-25) writes: "It is established practice in model making to design the model in accordance with the best indications of theory and then modify the finished model so that it will behave as the prototype is known to behave from field data".

Such modifications account for this report.

TABLE OF CONTENTS

INTERIM REPORT

Mechanical Alterations to Alberni Harbour Model

by

R.A. Pollard

INTRODUCTION

A hydraulic model of Alberni Harbour was built during 1950 and 1951 by Nuttall (1,2) at the Pacific Biological Station, Nanaimo, B.C.

Alberni Harbour is situated at the head of Alberni Inlet, a thirty-mile long fiord on the west coast of Vancouver Island. The Somass River, the largest discharging into the inlet, enters the north end of the harbour. The model covers the area north of Polly Point, about two miles long by one mile wide.

Its scales are:

Horizontal	$\frac{1}{1000}$
Vertical	$\frac{1}{84}$
Time	$\frac{1}{109}$

Fresh water entering the prototype from the Somass River spreads over the surface entraining sea water enroute to form a brackish upper zone which becomes more saline to seaward. There exists a vertical salinity gradient everywhere in the harbour, the salinity increasing with depth because fresh water is lighter than salt water. Where the brackish upper zone bounds the saline deep zone the salinity increases rapidly.

In the model fresh water flows down the Somass into the harbour, while sea water enters during the flooding tide and mixed fresh and sea water leaves during the ebbing tide at the seaward end. The water level in the model rises and falls to duplicate the tides. The model tides are predicted by a four-component Kelvin machine. These predictions are fed to a pair of sleeve valves which control the rate of injection of salt water and of extraction of mixed water from the model. One valve, the inlet valve, admits salt water to the model during the flood; the other, the outlet valve, removes mixed water during the ebb. A standpipe with two orifices controls the

proportion of surface water and deep water leaving the model through the outlet valve.

In the summer of 1941 the Pacific Oceanographic Group conducted an oceanographic survey of Alberni Inlet and Alberni Harbour, the results of which have been thoroughly analyzed by Tully (3). Among the data gathered on this survey were the gradients of salinity with depth. It is our objective to reproduce in the model at the same locations, at the same stage of the tide, at the same Somass discharge, and with the same past history of tide and river, the salinity gradients found in the prototype.

This report treats the physical alterations to the model in search of this goal. A sequel entitled Verification of the Alberni Harbour Model will follow.

COORDINATES

Black lines of latitude and longitude comprising the grid by which Alberni Harbour was divided in the 1941 oceanographic survey have been painted on the model. This is the grid, for identifying the plan position of sampling stations, shown in Figure 2 of Oceanography and Prediction of Pulp Mill Pollution in Alberni Inlet (3).

Grid line 4-5 lies along latitude 49° 15' N. Grid line G-H lies along longitude 124° 50' W. Each square is 507 feet by 507 feet.

HEADWORKS

In the river headworks the Somass water flows first into a tank, 2.7 ft long by 1.6 ft wide, where its velocity is reduced almost to zero, and discharges then through a 30-degree triangular weir into the model. The flow is controlled manually with a globe valve in the one-inch pipe supplying the tank. (Through such a valve is the best plumbing fitting on the market for regulating the flow of water, it is still far from satisfactory.) The discharge is measured from the head over the weir.

The Somass River flow into the model varies between 0.00024 cfs and 0.0192 cfs, corresponding to 185 cfs and 14,800 cfs in the prototype. The weir chosen was triangular because this shape enables the accurate measurement of the low flows without necessitating an unduly deep reservoir to handle the freshets, the accuracy of the discharge depending upon the accuracy with which the head is measured. For a triangular weir the discharge is

$$Q = c \frac{8}{15} \tan \frac{\theta}{2} \sqrt{2g} \, H^{\frac{5}{2}} \qquad (1)$$

where c is a coefficient to correct for friction and contraction. For a given small error ΔH in measuring the head the resulting error ΔQ in the discharge is proportional to $Q^{\frac{1}{2}}$. Hence the percentage error in Q due to a given error in H is greatest at the lowest flow. In order to calculate Q within five percent the head must be measured within 0.01 inch.

During experiments the Somass River flow is changed daily at midnight, which occurs every 13.2 minutes in the model. A quick way of accurately measuring the discharge had to be devised. The idea of a hook gauge to measure the head directly was discarded in favor of a device to magnify the head physically in order that the "magnified head" might be read less painfully without sacrificing accuracy.

Figure 1 shows the open oil manometer originally installed to magnify the head.

If s = specific gravity oil

d = diameter manometer tube

D = diameter oil reservoir

then $$\Delta Z_1 = \left[1 + s\left(\frac{d^2}{D^2} - 1\right)\right] \Delta Z_2 \quad . \qquad (2)$$

If s = 0.8, then the magnification of a change in head ΔZ_1 over the weir is four. Unfortunately this manometer, fine in theory, was useless in practice because the oil responded too sluggishly to the sudden changes in head during the experiments.

The visual multiplication scheme shown in Figure 2 was substituted. Here the bottom of the meniscus in the piezometer is sighted against a scale on the laboratory wall whence the prototype discharge is read directly. The peep hole and the weir notch are on the same level. The magnification

$X = \frac{318.2}{32.65} = 9.75$. The capillary rise in the tube h = 0.11 inch and is constant. Hence the zero mark on the scale falls 1.1 inch above the datum. The scale was constructed as follows.

Under heads of roughly one, two, and three inches, the water discharging through the weir at a steady flow was timed and weighed. At each of the three levels the line of sight was marked on the wall. The values XH measured on the wall were used to calculate three values of c in Equation 1. These ranged from 0.66 to 0.63. Using an average value of c values of XH corresponding to integral values of Q were calculated and plotted on the scale.

SERVO CONTROL MECHANISM

A mercury pot sits atop a float which follows the water level in the model. Three rigidly separated probes, each about one thirty-second inch apart in elevation, are mechanically lined to the tide computer; the trio moves vertically up and down following the computed tide height such that the water level in the model is correct when the middle probe is just touching the mercury. The circuit is designed to supply 40 volts to the servo-motor when all three probes are either clear of the mercury or immersed in it, and 30 volts when the long probe only or the long and middle probes both are immersed. Since the servo-motor is series-wound a reduction in the voltage supply reduces its speed. If all three probes are out of the mercury, the model tide being far too low, the servo-motor turns clockwise, thereby increasing the opening of the inlet valve and decreasing the opening of the outlet valve a like number of degrees. When the long probe touches the mercury, the model tide being now only slightly too low, the motor reduces speed, still turning clockwise. When the middle probe touches, the model tide being slightly too high, the motor reverses direction at the same reduced speed, thereby decreasing the opening of the inlet valve and increasing the opening of the outlet valve. When all three probes are immersed, the model tide being far too high, the motor speeds up, turning counter-clockwise. Thus does the surface of the mercury hunt for the middle probe.

The $\frac{1}{15}$ - hp motor originally installed, to bias the opening of the inlet and outlet valves when the water level in the model differs from the computed level, turned too slowly. The water level in the model frequently would err as much as one quarter inch (1.7 feet in the prototype) and take two or more minutes (3.6 hours in the prototype) to recover.

A more powerful servo-motor, recommended by Fjarlie, which could turn faster and thereby more rapidly throw upon the valve openings the bias dictated by the control probes, was installed. The new motor will change the bias from zero to eight degrees, or 31 percent of the valve opening corresponding to an absolute maximum rate of change of tide height (3.0 feet per hour in the prototype), in four seconds (7 minutes in the prototype). Thereafter the bias will remain constant and the water level will recover at the rate of one quarter inch in 67 seconds until the middle probe touches the mercury.

The electrical circuit, which had to be modified slightly, is shown in Figure 3.

MODIFICATION OF THE COMPUTED TIDE [1]

Since the magnitude of the range of the tide in Alberni Inlet is a measure of the extent of tidal flushing, we, being suspicious of the limitations of the

---

1. All times mentioned in this report are Pacific Standard.

four-component equation, decided to analyze the range of the model tide.

A list of sixty-one harmonic constants of the tide at Port Alberni, furnished by the Canadian Hydrographic Service, is given by Nuttall (2, p. 10).

The tide computer in the laboratory predicts both the tide height and the rate of change of tide height at Port Alberni, using the four components having the greatest amplitide of the sixty listed, namely, S_2, M_2, K_1, and O_1. The computer solves mechanically the following equations for the tide height and rate of change of tide height:

$$\begin{aligned} H = Z_o &+ Z_{S2} \cos(a_{S2} t + \alpha_{S2}) \\ &+ Z_{M2} \cos(a_{M2} t + \alpha_{M2}) \\ &+ Z_{K1} \cos(a_{K1} t + \alpha_{K1}) \\ &+ Z_{O1} \cos(a_{O1} t + \alpha_{O1}) \end{aligned} \qquad (3)$$

$$\begin{aligned} \frac{dH}{dt} = &- \frac{\pi}{180} a_{S2} Z_{S2} \sin(a_{S2} t + \alpha_{S2}) \\ &- \frac{\pi}{180} a_{M2} Z_{M2} \sin(a_{M2} t + \alpha_{M2}) \\ &- \frac{\pi}{180} a_{K1} Z_{K1} \sin(a_{K1} t + \alpha_{K1}) \\ &- \frac{\pi}{180} a_{O1} Z_{O1} \sin(a_{O1} t + \alpha_{O1}) \end{aligned} \qquad (4)$$

where H = tide height in feet at any instant after some arbitrary initial epoch

Z_o = elevation of mean sea level in feet at Port Alberni above an arbitrary datum at the approximate level of lowest normal tides

Z = amplitude in feet of component tide

a = speed of component in degrees per mean solar hour

t = time in hours after initial epoch

α = phase angle of component tide at initial epoch

$\frac{dH}{dt}$ = rate of change of tide height in feet per hour

If we chose the initial epoch 0000 on January 1, 1941, and substitute the appropriate values of speed and phase angle (4) then the computer solves the following equations:

$$H = 6.451 + 0.876 \cos (30.0000000\ t - 24°.6) + 3.128 \cos (28.9841042\ t + 288°.9) + 1.300 \cos (15.0410686\ t - 116°.1) + 0.809 \cos (13.9430356\ t + 165°.2) \quad (5)$$

$$\frac{dH}{dt} = - 0.459 \sin (30.0000000\ t - 24°.6) - 1.582 \sin (28.9841042\ t + 288°.9) - 0.341 \sin (15.0410686\ t - 116°.1) - 0.197 \sin (13.9430356\ t + 165°.2) \quad (6)$$

When the phase angle of every component in the harmonic equation of a tide equals zero then the height is an absolute maximum; likewise when the phase angle of every component equals 180 degrees then the height is an absolute minimum. Table 1 gives these absolute extremes from the four-component equation of the tide at Port Alberni and from the sixty-component equation, which, in the absence of wind, would yield a close replica of the actual tides. The mean height (mean sea level) of both the four-component tide and the sixty-component tide above the tidal datum is necessarily the same, namely 6.451 feet.

TABLE I

ABSOLUTE EXTREMES AT PORT ALBERNI FROM THE HARMONIC CONSTANTS

	FOUR COMPONENTS	SIXTY COMPONENTS
Absolute maximum height	12.564	15.754
Mean sea level	6.451	6.451
Absolute minimum height	0.338	- 2.852
Absolute maximum range	12.226	18.606

If the model is geared to reproduce implicitly the tides predicted by the computer then the model tide can never rise as high as the highest tides in the prototype nor can it ever fall as low as the lowest.

It is interesting to note in the tide tables (5) the annual highest and lowest tides predicted for Clayoquot, B.C. The "tidal differences" in the 1952 tide tables imply that the extreme Port Alberni heights equal the extreme Clayoquot heights. Table 2 lists the annual extremes predicted in the tide tables for Clayoquot. Included for comparison are the annual extremes recorded at Clayoquot (6). The highest tide ever recorded at Clayoquot was 15.2 feet, in 1920. Twenty-four harmonic components of the tide at Clayoquot are used in the tide-table predictions.

TABLE 2

ANNUAL EXTREMES AT CLAYOQUOT B.C.

YEAR	HIGHEST TIDE		LOWEST TIDE	
	Predicted	Recorded	Predicted	Recorded
1932	13.9	14.6	0.2	-0.3
1933	13.5	14.7	-0.1	-0.2
1934	13.5	14.0	0.0	-0.4
1935	13.4	14.2	0.4	-0.2
1936	13.7	14.2	0.2	-0.6
1937	13.6	14.6	-0.1	-0.4
1938	13.5	14.1	0.2	-0.1
1939	13.6	14.9	0.4	-0.1
1940	13.6	14.1	0.5	0.1
1941	13.7	15.1	0.1	-0.5
1942	13.6	13.7	0.1	-0.7
1943	13.9	13.4	0.2	-0.5
1944	13.6	14.1	0.5	-0.2
1945	13.7	13.7	0.1	-0.4
1946	13.9	14.0	-0.2	-0.9
1947	13.8	14.1	-0.2	-0.7
1948	13.6	14.5	0.1	-0.4
1949	13.5	13.6	0.2	-0.6
1950	13.7		-0.2	
1951	13.7		-0.2	
1952	13.4		0.0	

This information verifies our deduction that the four-component tide, which can never exceed 12.564 feet, will not usually attain the extreme heights of the prototype.

The range of a tide is the difference in elevation between a high water and the succeeding low or between a low water and the succeeding high. We define the "mean range" of the tide as the arithmetic mean of its individual ranges over a complete tidal cycle. Though actually the tides never repeat themselves, such a cycle may be assumed to recur every 18.6 years, the period of the obliquity of the moon's orbit. Over a complete tidal cycle the mean range equals the mean of the maxima minus the mean of the minima. We define the "average range" of the tide as the average of its individual ranges during a finite interval of time. See Figure 4.

By judiciously selecting the interval, one can obtain, in its average range, a close approximation of the mean range. Accordingly we have evaluated the average range of the tide at Clayoquot from the tide-table predictions during an interval of twelve consecutive lunar months in 1941. This 1941 average-range is 7.00 feet and is presumed to be the mean range of the tide at Clayoquot.

Available for examining the ranges of the model tide was a curve of the four-component tide, traced by the tide recorder, from January 1 to May 26, 1941. Starting with the first quarter on January 5 and ending with the new moon on May 25, we compared the average range of the four-component tide with that of the tide-table predictions during twenty separate lunar days - at five first quarters, five full moons, five third quarters, and five new moons. Intuitively we assumed that the ratio between the average ranges, for any interval whatever, of the four-component tide and the tide-table predictions would equal the ratio between the mean ranges themselves.

This short-cut analysis showed the average range of the four-component tide to be 5.65 ft and of the predictions to be 6.60 ft. Thus the ratio between the mean range of the model tide and of the prototype tide was assumed to be $\frac{5.65}{6.60}$, or $\frac{1}{1.17}$. That is, as long as the model remained geared to reproduce implicitly the tide predicted by the four-component computer, the average of all ranges in the prototype tide would be 17 percent greater than the corresponding average in the model. Consequently the tide could not flush the fresh water from Alberni Harbour as effectively in the model as it does in the prototype.

It follows that we could improve the model tide by increasing its range by 17 percent. This could have been done by increasing the length of each height and each derivative crank on the tide computer by 17 percent, which is equivalent to increasing the amplitude of each of the four components, S_2, M_2, K_1 and O_1, by 17 percent. Because the lengths of the cranks on our tide computer are not adjustable, the same result was accomplished by shifting the position of the connections to the height arm of both the probes and the recorder pen such that the distance from each connection to the pivot was 17 percent greater. Whereas the model previously had reproduced the

tides dictated by the equation,

$$H = Z_o + \sum_{n=4}^{\text{components}} Z_n \cos(a_n t + \alpha_n), \qquad (10)$$

it now obeys the modified equation,

$$H = Z_o + 1.17\left[\sum_{n=4}^{\text{components}} Z_n \cos(a_n t + \alpha_n)\right]. \qquad (11)$$

The results shown in Figure 5 justify this modification. From left to right are plotted the frequency distributions of both high and low waters for the following tides during the intervals specified.

1. Tide-table Predictions for Clayoquot During Twelve Consecutive Lunar Months in 1941.

The average range is 7.00 ft. If this interval be assumed representative of a complete tidal cycle, then the mean range also is 7.00 ft.

2. Tide-table Predictions for Clayoquot and Four-component Tide at Port Alberni from January to May, 1941.

From the tide tables the average range is 6.95 ft; from the four-component equation the average range is only 5.84 ft. The ratio between the two is $\frac{1.19}{1}$.

3. Tide-table Predictions for Clayoquot and Modified Four-component Tide from April to June, 1941.

From the tide tables the average range is 6.96 ft; from the modified four-component equation the average range is 7.05 ft - approximately equal. Hence the ratio is now unity.

The information given in the tide tables for converting Clayoquot heights and times into Port Alberni heights and times is meagre. According to the table of "tidal differences" in the tide tables, the "mean ratio of rise" of the maxima at Port Alberni is 98 percent of the maxima at Clayoquot. Presumably, therefore, we are justified in comparing the model tides at Port Alberni with the predictions for Clayoquot.

In conclusion, the fidelity of the tide computed by a Kelvin machine utilizing only a very few of the harmonic components of the tide can be improved by increasing the amplitude of each component on the machine in the ratio of the mean range of the prototype tide to the mean range of the tide given by those few components.

ERRORS IN THE TIDE COMPUTER AND RECORDER

One pen of the tide recorder traces a curve of the computed tide, or modified computed-tide; the other traces the actual water level in the model. The paper is driven at one inch per minute by a $\frac{1}{15}$ - hp motor. Time intervals corresponding to one hour in nature are marked on the paper by a selsyn motor electrically coupled to a selsyn generator turned by the tide computer. Figure 6 shows how these pens are actuated.

The computed-height pen reciprocates on top of the paper in a straight slot recording the motion up and down of the height arm, to which it is directly connected by a wire.[1] The photograph of the tide recorder (Figure 7) shows the graph of the computed-tide height being traced. At the instant the picture was taken the model time was 1500 on April 23 and the computed-tide height indicated was 3.2 ft. Notice how the curve is flattened at high water and low water due to friction in the pulleys of the height-integrating cable, an error discussed later in detail.

The tide-computing machine mechanically solves the four-component equation for the tide height. The solution of this equation appears on the tide recorder as a graph of tide height versus time. However there usually is a discrepancy between this recorded height and the mathematically calculated height of the four-component tide at any particular instant. The mathematical solution of the four-component equation is the correct one. The recorded tide-height is in error from the following causes. The elevation of the probes, which dictates the model water-level, will be in error from the first four of these. A positive error signifies that the tide is too high.

1. Inexact Gear Ratios Between the Four Components in the Tide Computing Machine.

At the sacrifice of accuracy, simple gear ratios between the components have been used in order that the gears themselves may be both small and few. The speed of any one component in the computer is governed by the sum of the gears motor-ward of that component. Beginning at the motor end of the computer, the components are driven in the order, S_2, M_2, K_1, and O_1. The S_2 component is driven at the correct speed. Thereafter each component suffers a constant error in speed. It follows that, if the computer is started at some epoch with all its components in correct phase, the phase of

---

1. Originally a waxed silk fishing line had been used to connect this pen to the height arm but this was discarded in favour of a fine stainless-steel wire. The fishing line was unsuitable because its length responded erratically to changes in both temperature and humidity, because it behaved inelastically to changes in tension, and because it was frayed by the pulleys. The only defect apparent in the existing connection is the wire's change in length with temperature, which is both small and calculable.

each of the components, M_2, K_1, and O_1, will steadily err. This will throw the tide height in error. The error in height resulting from the inexact gear ratios after one year will vary from zero to plus or minus 0.9 ft. Table 3 shows the error in speed of each component and its contribution to the greatest possible error in tide height.

TABLE 3

ERROR IN SPEED OF COMPONENTS IN TIDE COMPUTER

COMPONENT	CORRECT SPEED	ACTUAL SPEED	ERROR IN SPEED	ERROR IN SPEED	MAXIMUM ERROR IN TIDE HEIGHT AFTER ONE YEAR
	Degrees/Hour	Degrees/Hour	Degrees/Hour	Percent	Feet high or low
S_2	30.000000	30.000000	0	0	0
M_2	28.984104	28.983051	0.001053 Slow	0.00363 Slow	0.6
K_1	15.041069	15.040480	0.000589 Slow	0.00392 Slow	0.1
O_1	13.943036	13.944067	0.001031 Fast	0.00739 Fast	0.2

2. Deviations from Parallel of the Integrating Cables.

Our system of summing the component-tide heights by means of cables requires that the cable span be long compared with the lengths of the cranks (amplitudes of the components). The deviations from parallel of the integrating cables, due to the displacement of the cranks, cause an error in the tide height such that the tide is always too low. The greatest error from this cause is minus 0.1 ft.

3. Temperature Changes in the Integrating Cables.

The length of the integrating cable is adjustable at its anchor. Once adjusted to be correct at a given temperature, a 6°F rise will make the tide 0.1 ft too high. We are prepared to keep adjusting the cable length if the temperature in the laboratory cannot be held constant.

4. Friction in the Pulleys.

If the pulleys were frictionless the tension in each of the eight parts of the integrating cable would be equal, and hence the sag in each part and the stretch in each part would be equal. Such is the ideal. Friction in the pulleys, however, causes the tension in each part to differ. The pulley friction factor is 0.07. That is, the tension in a cable is changed by 7 percent in passing through 180 degrees over a pulley. During the ebb, when the cable is lifting the height arm, the tension in the anchored part is 72 percent greater than the tension at the free end, the sag is 42 percent less than the ideal, and the stretch is 37 percent greater than the ideal. In each of the eight parts the tension exceeds

that at the free end, the sag is less than the ideal, and the stretch exceeds the ideal. The sum of the decrements in sag causes an error in the tide height of plus 0.1 ft; the sum of the increments in stretch an error of plus 0.1 ft also. Thus during the ebb the tide is constantly 0.2 ft too high due to pulley friction. Likewise during the flood, when the cable is lowering the height arm, the tension in each of the eight parts decreases progressively toward the anchored end, the sag exceeds the ideal, and the stretch is less than the ideal. As a result the tide height is in error minus 0.2 ft due to sag and minus 0.1 ft due to stretch. Thus during the flood the tide is constantly 0.3 ft too low due to pulley friction. Figure 8 shows the effect of pulley friction upon the recorded graph of the computed tide. The friction could be reduced by the use of ball-bearing pulleys.

5. Temperature Changes in the Wire Connecting the Pen to the Height Arm.

The recorded tide-height is subject to an error due to thermal expansion of the wire connecting the pen to the height arm. Once its length has been adjusted to be correct at a given temperature, a 24°F rise will make the recorded tide 0.1 ft too low.

6. Play Between the Moving Paper and its Guides.

There is room for play between the moving paper and its guides amounting to a random error in the recorded tide-height from zero to minus 0.2 ft.

The foregoing errors in the recorded tide are summarized in Table 4.

To check the accuracy of the tide computer and recorder combination, the instantaneous value of H from the four-component equation was mathematically solved at seven epoches during the run from January to May, 1941, and its value from the modified four-component equation at six epochs during the run from April to June, 1941. These values are compared in Table 5 with the values of H at the same instants drawn by the recorder pen. Nowhere is the discrepancy between recorded H and calculated H excessive in view of the preceding analysis.

ERRORS IN THE WATER LEVEL RECORDER

The water-level pen reciprocates on the opposite side of the paper directly underneath the computed-height pen, recording the actual water level in the model by a direct connection to a float. Whereas an unfettered float would subserviently follow every rise and fall of the water in the model, pulley friction and surface tension preclude that precision when the float is tied to the recorder. Figure 9 shows the system used to actuate the water-level pen.

TABLE 4

SOURCES OF ERROR IN THE RECORDED TIDE

SOURCE OF ERROR IN RECORDED TIDE AND MODEL WATER LEVEL BOTH	ERROR IN TIDE HEIGHT IN FEET	NATURE OF ERROR
1. Inexact gear ratios	up to 0.9 high or low after one year	Random and increasing with time
2. Deviations from parallel	up to 0.1 low	Random
3. Temperature in cables	0.1 high per 6°F rise 0.1 low per 6°F drop	Proportional to temperature change
4. Friction in pulleys	0.2 high during ebb 0.3 low during flood	Constant
SOURCE OF ERROR IN RECORDED TIDE ONLY		
5. Temperature in wire	0.1 low per 24°F rise 0.1 high per 24°F drop	Proportional to temperature change
6. Play in guides	up to 0.2 low	Random

TABLE 5

VALUES OF H FROM FOUR-COMPONENT EQUATION

DURING RUN FROM JANUARY 1, TO MAY 26, 1941

INSTANT		RECORDED H FEET	CALCULATED H FEET	ERROR FEET
0000	January 1	7.1	6.91	0.2 high
0000	February 1	6.7	6.31	0.4 high
0000	March 1	8.8	8.77	0.0
0000	April 1	7.9	8.17	0.3 low
0000	April 11	10.7	10.88	0.2 low
0000	May 1	7.5	7.94	0.4 low
0000	May 11	11.6	11.40	0.2 high

VALUES OF H FROM MODIFIED FOUR-COMPONENT EQUATION

DURING RUN FROM APRIL 1 TO JUNE 22, 1941

INSTANT		RECORDED H FEET	CALCULATED H FEET	ERROR FEET
0000	April 1	8.4	8.46	0.1 low
0000	April 11	11.4	11.63	0.1 low
0000	May 1	8.5	8.19	0.3 high
0000	May 11	12.2	12.25	0.0
0000	June 1	6.2	5.81	0.4 high
0000	June 23	11.4	11.29	0.1 high

The recorded water-level is subject to error from:

1. Friction in the Pulleys.

2. Surface Tension.

3. Elasticity of the Cord.

4. Variations of the Water Density.

If the surface of the float were such that the shape of the meniscus remained constant whenever the water level accelerated up or down relative to the float, and if the cord were inextensible, and if also static and dynamic pulley friction were equal, then the drop or rise in water level necessary to start the pulleys moving is

$$\Delta h = \frac{8.66 \times C}{w A} \qquad (12)$$

where Δh = drop in water level

X = friction factor, assumed to be small. for a cord passing through 180° over a pulley

C = weight of counterweight

w = specific weight water, assumed constant

A = plan area of float

This value of Δh in the model amounts to 0.3 feet in the prototype (Figure 10).

The equation reveals that this error can be reduced by decreasing the pulley friction, by lightening the counterweight, or by using a bigger float - and by these three changes only. Ball-bearing pulleys would improve the friction factor. The counterweight must be heavy enough to hold the pen against the paper. Any float in the model offers an obstruction to the flows which is non-existent in the prototype; therefore a bigger float only increases this obstruction.

At first a wooden float was used. This was discarded because its weight would increase from absorption of water during the course of an experiment. The wooden float did yield a water-level trace which resembled the theoretical trace in error due to pulley friction alone. A waxed watertight metal float was substituted. Since this float is impermeable its weight remains constant. The trace from this float, however, showed not only the lag characteristic of pulley friction but also an erratic stepping. Figure 11 shows a typical trace.

Apparently the wooden-float trace was in error mainly from pulley friction, for no effects of surface tension, elasticity, or density were perceptible. It follows that, since the metal float was tied to the pen via the same system of pulleys, its stepped trace must be attributed to surface tension, and the effects of elasticity and density are negligible.

The effect of surface tension upon the wooden float was constant because the porosity of its surface assured the sides of the float remaining wet. The effect of surface tension upon the waxed float apparently depends upon the acceleration of the water level relative to the float. A visual examination of the meniscus when the unfettered float was depressed and raised from a freely floating position in a basin of water gave the results in Figure 12.

A possible explanation for the steps in the water-level trace follows. Consider the water initially rising very slowly at a steady rate. The float is in equilibrium with the water (Case 1). The trace is smooth but lags the actual water level due to pulley friction. Now let the water rise at an accelerated rate. Because of its inertia the float lags behind the water (Case 2). There now exists an unbalanced vertical force on the float whose magnitude is

$$F = (h_u - h_e)wA + (a_u - a_e)wl \ . \qquad (14)$$

The upward acceleration of the water relative to the float will sooner or later cease, whereupon this unbalanced force will catapult the float vertically up beyond the equilibrium draught h_e. The float will now oscillate vertically about the equilibrium draught. As soon as the float begins to move down as a result of its over-shooting the equilibrium draught - the absolute water level still rising - the trace will flatten. The trace will remain horizontal until the float again rises to the absolute elevation at which it started to drop - the absolute water level still rising.

Presumably these steps in the water-level trace could be eliminated by using a watertight float coated with a porous material. We have not tried such a float because an electronic water-level recorder similar to that designed by Lincoln at the University of Washington is presently under construction.

TITRATIONS

The apparatus shown in Figure 13 was used in the model laboratory to determine by the Mohr titration method the chlorinity of the water samples taken from the model. The apparatus and the procedure used are described by Tully (3, pp. 128-129).

THE EXCHANGE OF WATER THROUGH THE VALVES

The lower basin and inlet and outlet valves are equivalent to thirty miles of Alberni Inlet missing from the model. They are required to exchange correctly the water between Alberni Harbour and the Pacific Ocean.

The evolution of our present system of exchanging the water is a story of disappointment, from which the following significant advances will be recounted:

1. Alteration to the Inlet Flow.

2. Gate Ebb-standpipe Mark 1.

3. Gate Ebb-standpipe Mark 2.

4. Gate Ebb-standpipe Mark 3.

5. Sill Ebb-standpipe.

The ultimate goal is a model which will everywhere duplicate the salinity gradients found in the prototype under the same boundary conditions.[1] To this end our first objective was to match the depth of the upper brackish layer at station L 20 under average Somass River discharges.

Station L 20, which is situated in the middle of Alberni Harbour, was chosen because here were the salinity gradients most frequently measured in the prototype. The depth of the upper zone in the prototype at L 20 under steady average river discharges (about 2500 cfs) is four meters (3, Fig. 14a, p. 30).

Our second objective was to match the depth of upper zone at L 20 under naturally fluctuating river flows. Our final objective was to match the depth of upper zone at every station in the harbour under fluctuating flows.

The photograph (Figure 14) shows the present system for injecting sea water into the model during the flood. The water enters at the bottom of a diverging flume. By the time it reaches the open gate its velocity is low and any excess air entrained in the supply has had time to escape. Thus the water enters the model quiescently. The black baffle extends down four meters below low-water level to prevent sea water leaving the flume during the ebb where the upper brackish layer from the lower basin alone is supposed to discharge.

Hitherto the sea water entered the model at the spot marked X. There were two objections to this system, namely, that the inflow was directed in a jet toward the servo-control float stilling-well, and that the effervescence of the water entering the model violently mixed the deep water with the upper zone.

During the ebb the outlet valve removes a quantity of the mixed fresh and sea water from the model, which total quantity and its rate of discharge are dictated by the tide computer (derivative components). The valve, however, does not respect the identity of the water it discharges. The water leaving the model, before discharging through the outlet valve, flows first through a standpipe which differentiates between the volumes withdrawn from the brackish surface layer and from the saline deep water. Two types of ebb standpipes have been tried, gate standpipes and sill standpipes. A gate

---

1. Refer to page 2 of this report.

standpipe utilizes moving orifices to discharge calculable quantities of water from each of the two zones. A sill standpipe has fixed openings which induce a velocity profile during the ebb resembling the prototype.

Figure 16 illustrates gate ebb-standpipes mark 1, mark 2, and mark 3. All are constructed with two separate orifices - an upper orifice to discharge water from the brackish upper zone and a deep orifice to discharge water from the saline deep zone.[1] The orifices are designed to discharge the water from the model into the standpipe, with the water in the standpipe a constant small drop h below the water level in the model during the ebb.

The upper orifice is required to discharge water from the upper zone at a rate such that fresh water will neither accumulate in the model nor be depleted under a steady river flow.

If Q = rate of river flow

T = time interval between successive high waters

S_d = salinity of deep water

S_u = salinity of upper zone

V_u = volume discharged through upper orifice during interval $\frac{T}{2}$

then
$$V_u = QT \frac{S_d}{S_d - S_u} \quad . \tag{15}$$

The outlet valve is required (2, pp. 12-13) to discharge mixed water at a rate proportional to the rate of change of tide height, $\frac{dH}{dt}$.

If V_v = volume discharged through outlet valve during interval $\frac{T}{2}$

V_m = volume of model between high-water line and low-water line

then
$$V_v = V_m + QT \quad . \tag{16}$$

The volume discharged through the deep orifice during the interval $\frac{T}{2}$ is

$$V_d = V_v - V_u \quad . \tag{17}$$

---

1. Figure 17 shows (a) a typical salinity gradient and (b) the shape of the gradient assumed in the design of a gate standpipe. The "depth of upper zone" is defined.

Mark 1 has a stationary upper weir whose width, manually adjusted by means of a baffle, is maintained proportional to the river flow. The head over the weir varies with the tide height; consequently the volume discharged from the upper zone varies with every falling tide. The average volume discharged may be calculated approximately if a simple harmonic tide of an average amplitude be assumed. The deep orifice is controlled by a sliding gate attached to the derivative arm, which varies its area in proportion to $\frac{dH}{dt}$. Since the head on the deep orifice is equal at every depth the rate of discharge of the deep water is proportional to $\frac{dH}{dt}$.

It is desirable to have openings in the standpipe which will withdraw water from both the upper and deep zones at a rate proportional to $\frac{dH}{dt}$ because the discharge of the mixture through the outlet valve is so proportional. Mark 2 is designed to accomplish this. The upper zone discharges under a constant head through an orifice in a sliding gate attached to the height arm. The width of the upper orifice, controlled by another gate attached to the derivative arm, varies in proportion to $\frac{dH}{dt}$. The height of this orifice is maintained proportional to the river flow by two baffles adjusted symmetrically about the orifice centerline. The deep orifice is the same as that in mark 1. Mark 2 was discarded because the flow through the upper orifice was turbulent, and hence unpredictable, due to leakage between the sliding gates and the standpipe.

Mark 3 is photographed in Figure 15. The upper zone discharges under a constant head through an orifice in a sliding gate attached to the height arm. The rate of this discharge is constant during the ebb. The height of this orifice is maintained proportional to the river flow by two baffles adjusted symmetrically about the orifice centerline for river flows below 2500 cfs. The deep water discharges through an orifice whose area again, controlled by a sliding gate attached to the derivative arm, varies in proportion to $\frac{dH}{dt}$. This orifice is opened from the top downward - a reversal from marks 1 and 2. The top of the orifice lies five meters below low-water level. Since the orifice opens first and closes last at its top, fresh water which would otherwise accumulate in the model during a freshet has a means of escape. The deep orifice acts therefore as a safety valve which prevents the upper zone from staying too deep. The photograph (Figure 18) shows how mark 3 is actuated.

The model's reaction to the May 1941 freshet (3, Fig. 16) was tested with gate ebb-standpipe mark 3. The results are listed in Table 6.

Tully reasonably contends that since there are no sliding gates in Alberni Inlet in the prototype there should exist some fixed shape of standpipe which is hydraulically equivalent to the bottom topography of the inlet in controlling the efflux of the water from Alberni Harbour.

The shape of the sill ebb-standpipe is the shape of the salinity gradient in the prototype at station A at low water during steady average Somass River discharge (3, Fig. 1). The elevation of the standpipe is such that zero depth in the salinity gradient lies at low-water level in the model. This shape is assumed by Tully (3, p. 155) to be a criterion of the velocity profile at station A during the ebb.

TABLE 6

REACTION OF MODEL TO MAY 1941 FRESHET
USING GATE MARK 3 AND SILL MARK 1 EBB STANDPIPES

STATION	DATE	PST	DEPTH OF UPPER ZONE IN METERS		
			PROTOTYPE	GATE MARK 3	SILL MARK 1
L 20	June 4	0749	4.1	5.2	5.2
L 20	June 5	1535	4.1	4.9	5.6
L 20	June 6	0709	2.4	4.6	5.0
L 20	June 7	1243	6.2	4.7	4.5
Q 19	June 9	1016	4.5	4.1	3.4
L 20	June 9	1230	6.1	4.0	3.2
H 23	June 9	1456	6.3	4.0	3.9
Q 19	June 10	0503	6.1	4.8	4.0
L 20	June 10	0711	6.2	4.5	
G 21	June 10	0921	4.1	4.1	3.3

The photograph (Figure 19) shows the sill ebb-standpipe with two sliding baffles, assembled on the left, and dismantled on the right. The baffles are intended for adjusting the proportions of water withdrawn from the two zones. The curves are the results of a test to determine the effect of moving the baffles upon the depth of upper zone. Evidently the depth of the upper zone in the model is decreased by raising the sill and increased by widening the deep slot. The second effect is reasonable.

From the calibration curves a baffle setting was interpolated which was expected to yield (dotted curve) a four-meter depth of upper zone at L 20 under a steady 2500-cfs Somass discharge. With this setting the model's reaction to the May 1941 freshet was tested. The results are listed in Table 6 alongside the equivalent for the gate ebb-standpipe mark 3.

Subsequent experiments in the model utilize gate ebb-standpipe mark 3.

References

1. Nuttall, J.B. Hydraulic model of Alberni Harbour. MSS. Rept., Joint Committee on Oceanography, Pacific Oceanographic Group, Nanaimo, B.C. December 1, 1950.

2. Nuttall, J.B. Report on construction. Hydraulic model of Alberni Harbour. MSS. Rept., Joint Committee on Oceanography, Pacific Oceanographic Group, Nanaimo, B.C. December 1, 1951.

3. Tully, J.P. Oceanography and prediction of pulp mill pollution in Alberni Inlet. Fish. Res. Bd. Can., Bull. 83. 1949.

4. Schureman, Paul. Manual of harmonic analysis and prediction of tides. Special Publication No. 98. U.S. Department of Commerce, Coast and Geodetic Survey, Washington, D.C. 1941.

5. Tide tables for the Pacific coast of Canada. Tidal Publication No. 10, Canadian Hydrographic Service, Department of Mines and Technical Surveys, Ottawa. 1932 to 1952.

6. Tide levels and tidal bench marks. Tidal Publication No. 30, Canadian Hydrographic Service, Department of Mines and Technical Surveys, Ottawa. 1951.

7. von Arx, W.S. Synoptic models of the circulation in estuaries. Proceedings of the Colloquium on the Flushing of Estuaries, Woods Hole Oceanographic Institution, Cambridge, Mass. 1950.

Additional Reference

Doodson, A.T., and H.D. Warburg. Admiralty manual of tides. H.M. Stationery Office, London. 1941.

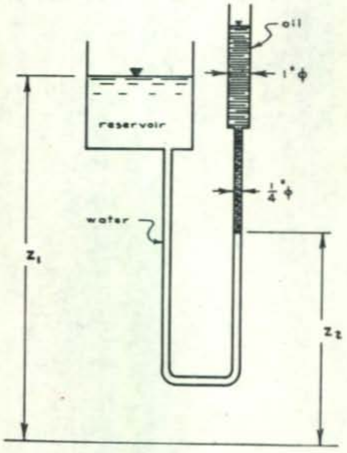

MANOMETER
MAGNIFICATION

Figure 1

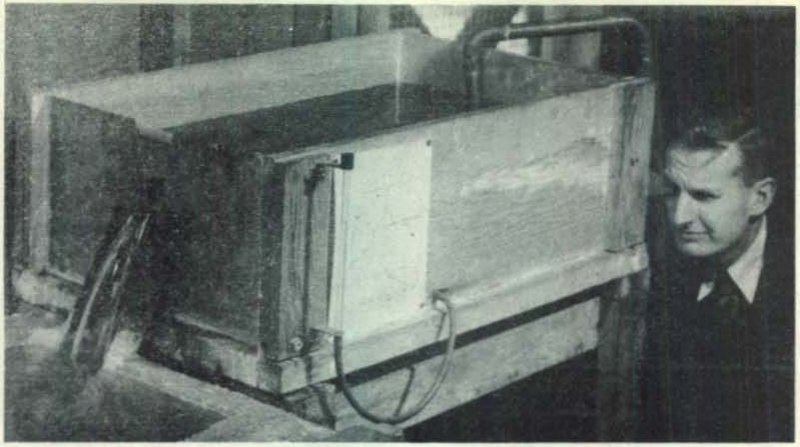

HEADWORKS

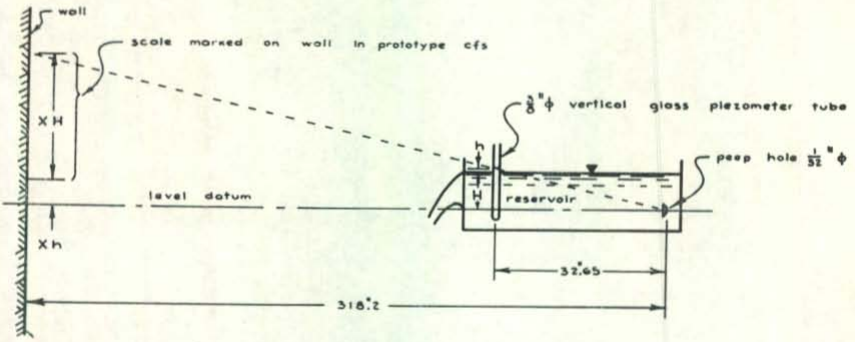

VISUAL MAGNIFICATION

Figure 2

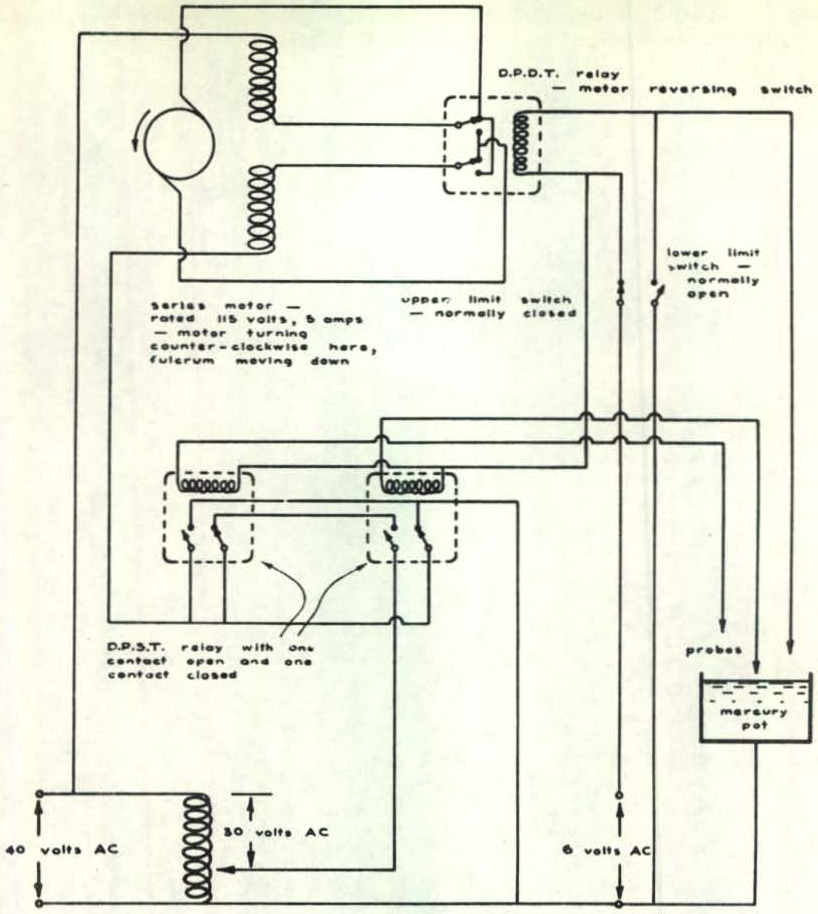

SERVO CONTROL CIRCUIT

Figure 3

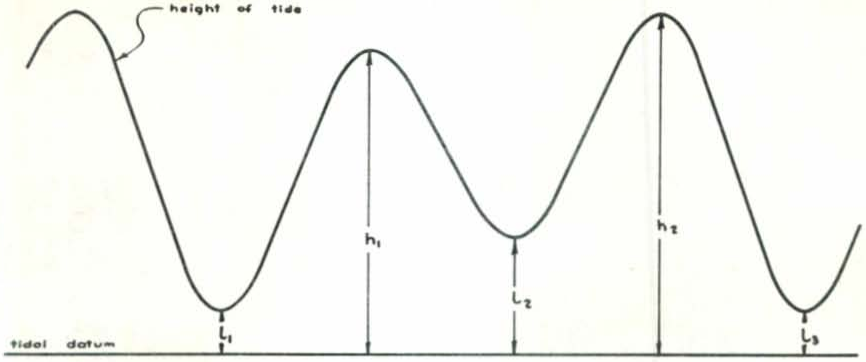

$$\text{Range} = h_1 - L_1 \quad \text{or} \quad h_1 - L_2 \tag{7}$$

$$\text{Mean Range} = \frac{\sum_{n \to \infty} h_n}{n} - \frac{\sum_{n \to \infty} L_n}{n} \tag{8}$$

$$\text{Average Range} = \frac{h_1 + h_2}{2} - \frac{L_1 + L_2}{2} \tag{9}$$

DEFINITIONS

Figure 4

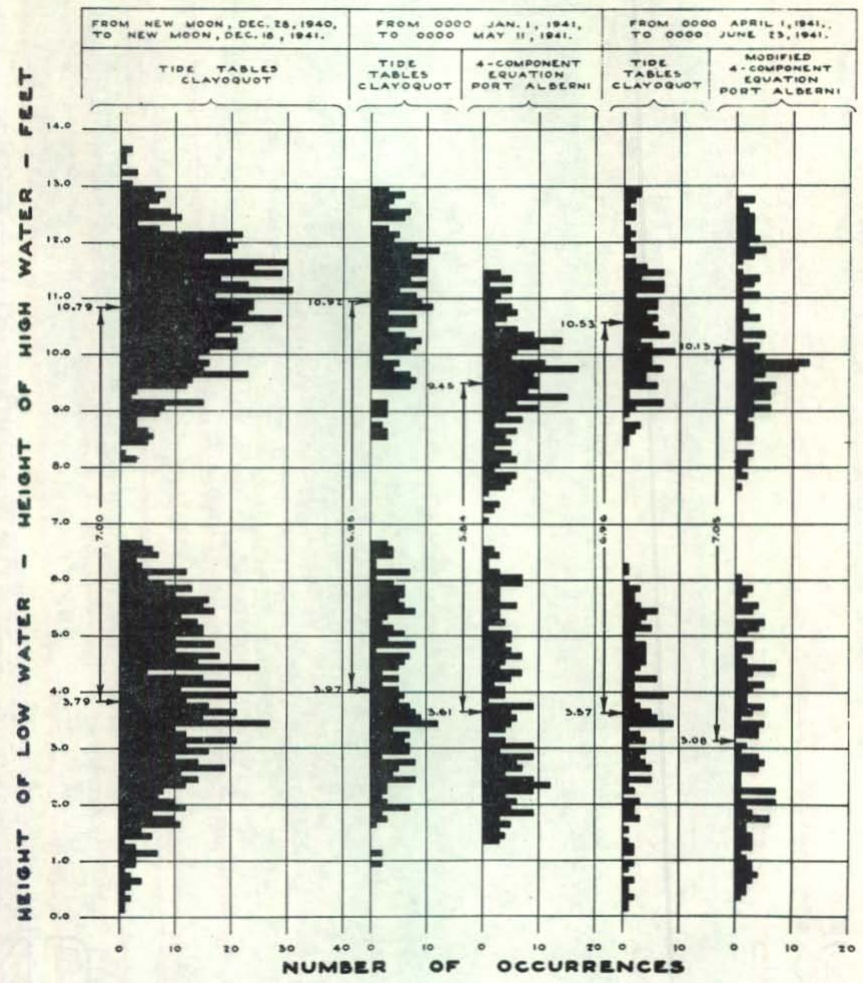
FREQUENCY DISTRIBUTION
OF
HIGH AND LOW TIDES
SHOWING MEAN EXTREMES AND AVERAGE RANGES
FROM NEW MOON, DEC. 28, 1940, TO NEW MOON, DEC. 18, 1941.
FROM 0000 JAN. 1, 1941, TO 0000 MAY 11, 1941.
FROM 0000 APRIL 1, 1941, TO 0000 JUNE 23, 1941.
TIDE TABLES CLAYOQUOT
TIDE TABLES CLAYOQUOT
4-COMPONENT EQUATION PORT ALBERNI
TIDE TABLES CLAYOQUOT
MODIFIED 4-COMPONENT EQUATION PORT ALBERNI
HEIGHT OF LOW WATER - HEIGHT OF HIGH WATER - FEET
14.0
13.0
12.0
11.0
10.0
9.0
8.0
7.0
6.0
5.0
4.0
3.0
2.0
1.0
0.0
10.79
10.92
10.53
10.13
9.45
7.00
6.96
6.84
6.96
7.06
3.97
3.79
3.61
3.57
3.08
0
10
20
30
40
NUMBER OF OCCURRENCES

Figure 5

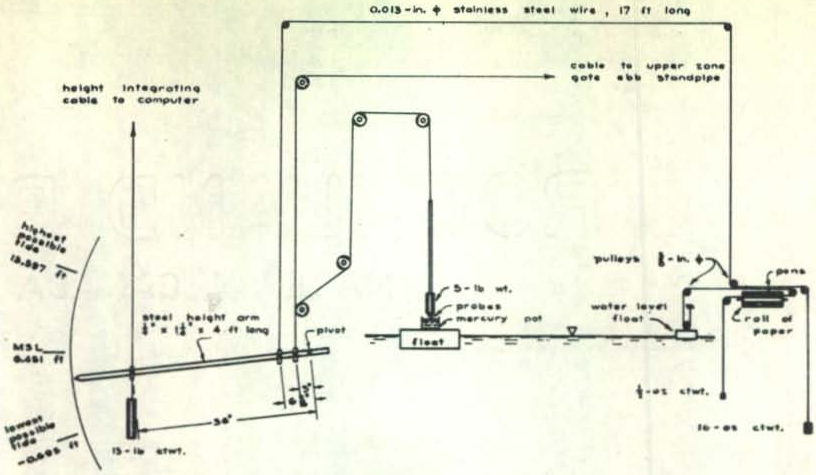

OPERATION OF TIDE RECORDER

Figure 6

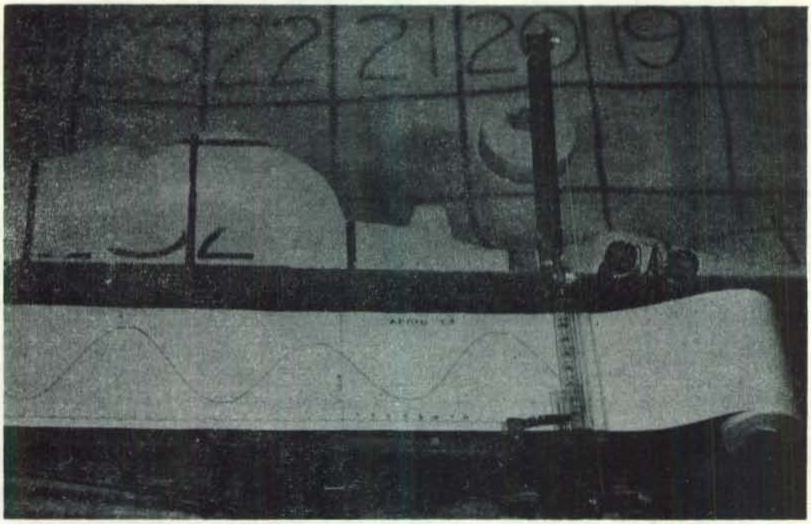

TIDE RECORDER

Figure 7

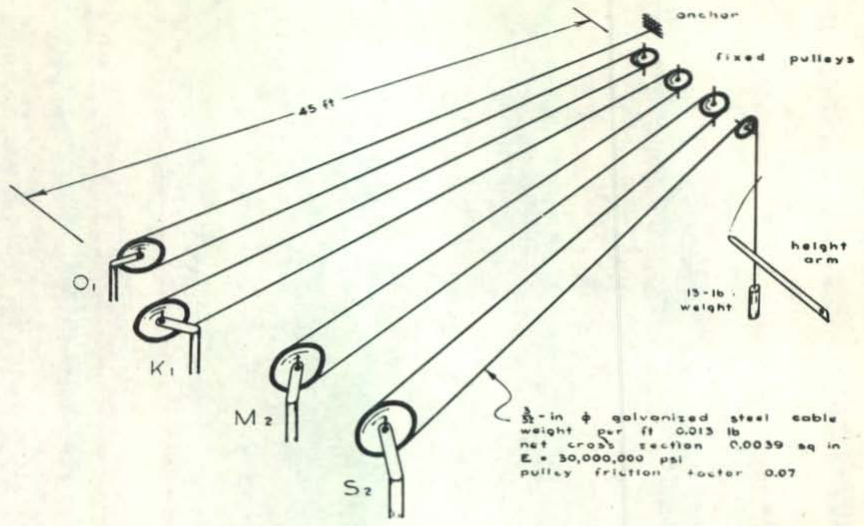

HEIGHT INTEGRATING CABLES

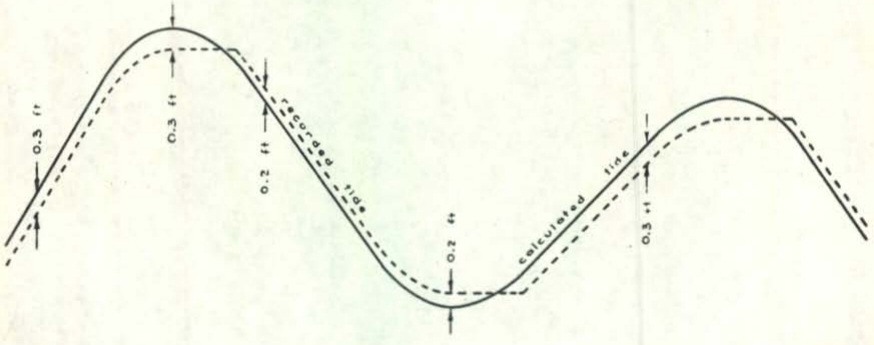

EFFECT OF FRICTION IN PULLEYS

Figure 8

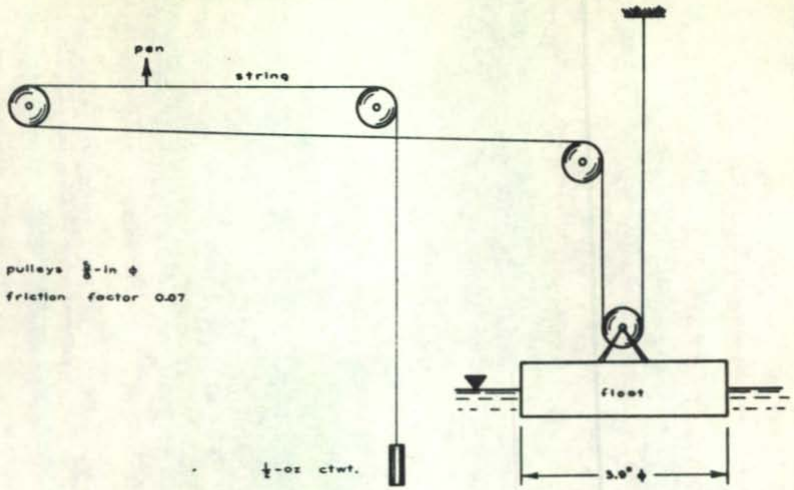

OPERATION OF WATER-LEVEL RECORDER

Figure 9

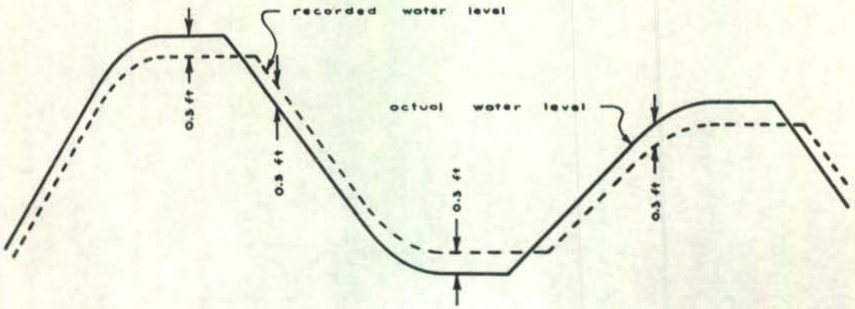

EFFECT OF FRICTION IN PULLEYS

Figure 10

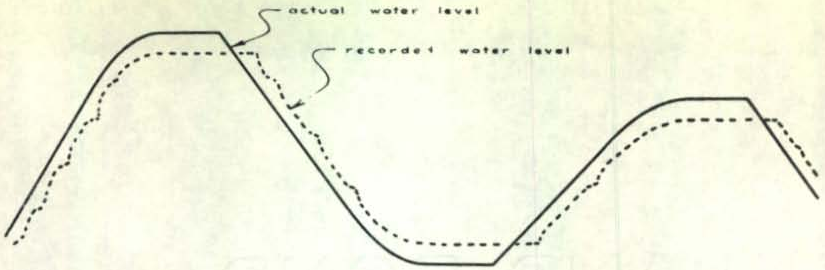

EFFECT OF SURFACE TENSION

Figure 11

1. FLOAT IN EQUILIBRIUM WITH WATER

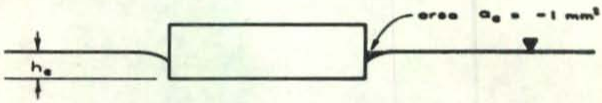

$$h_e = \frac{W}{wA} + \frac{a_e l}{A} \qquad (13)$$

where W = weight of float
w = specific weight of water
A = plan area of float
a = cross-sectional area of meniscus
l = perimeter of float

2. WATER ACCELERATING UP

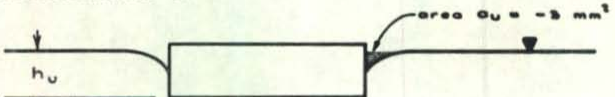

$h_u > h_e$
$a_u < a_e$

3. WATER ACCELERATING DOWN

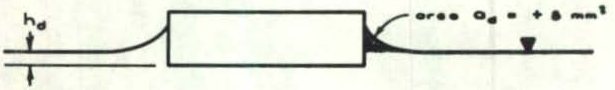

$h_d < h_e$
$a_d > a_e$

SHAPE OF MENISCUS

Figure 12

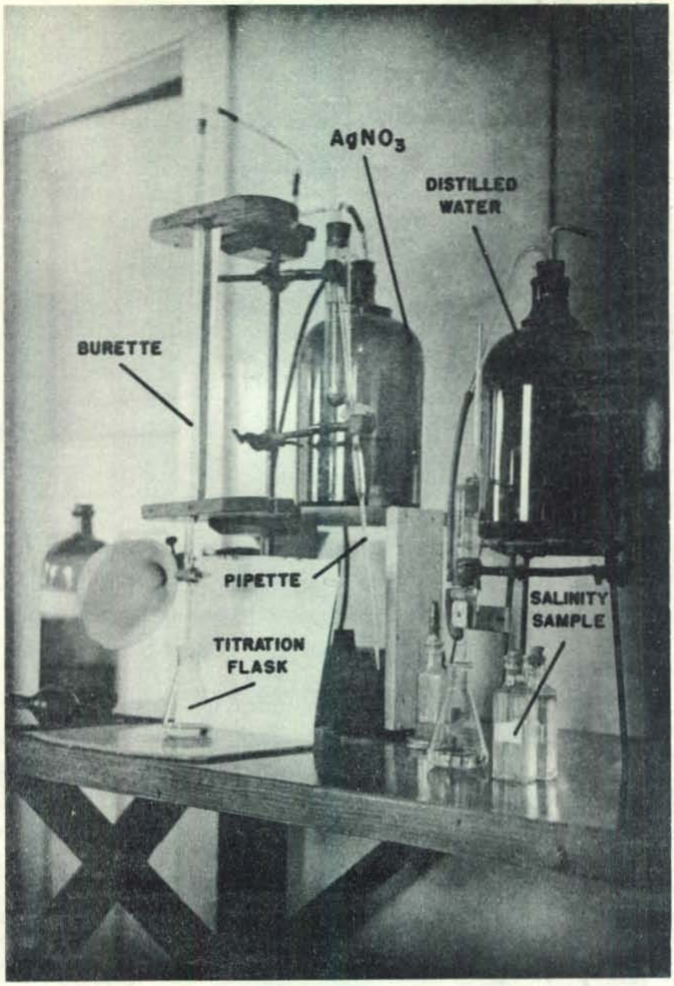

CHLORIDE TITRATION APPARATUS

Figure 13

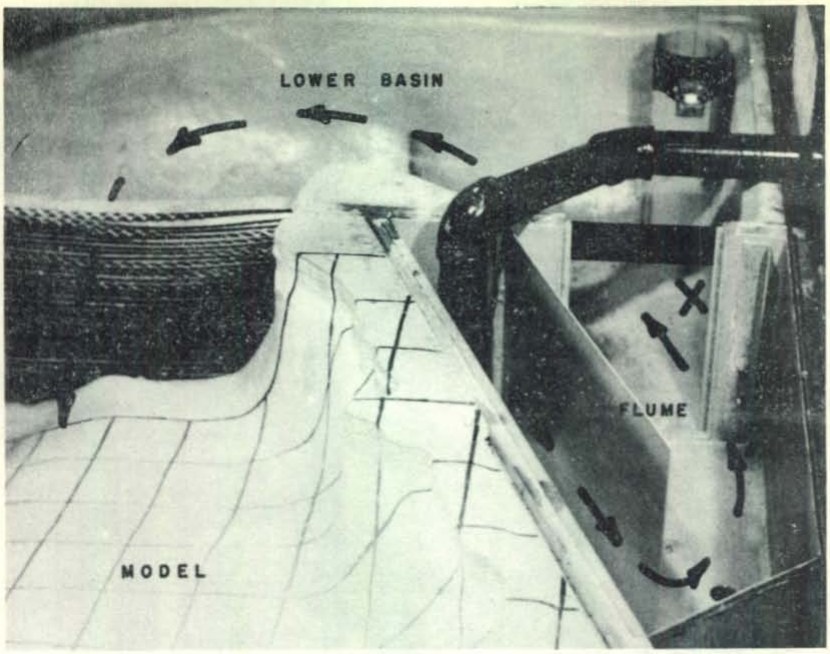

INLET FLOW

Figure 14

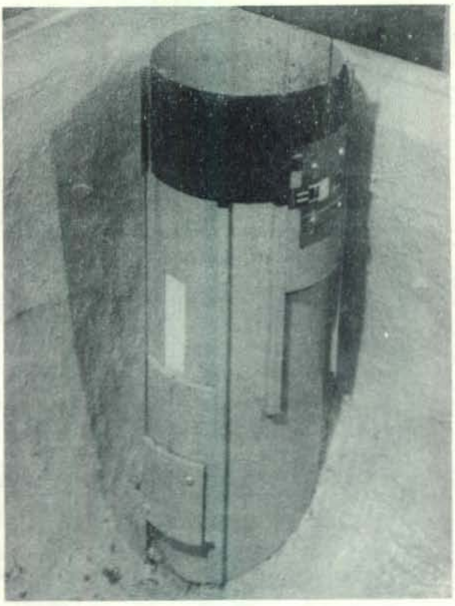

GATE EBB-STANDPIPE MARK 3

Figure 15

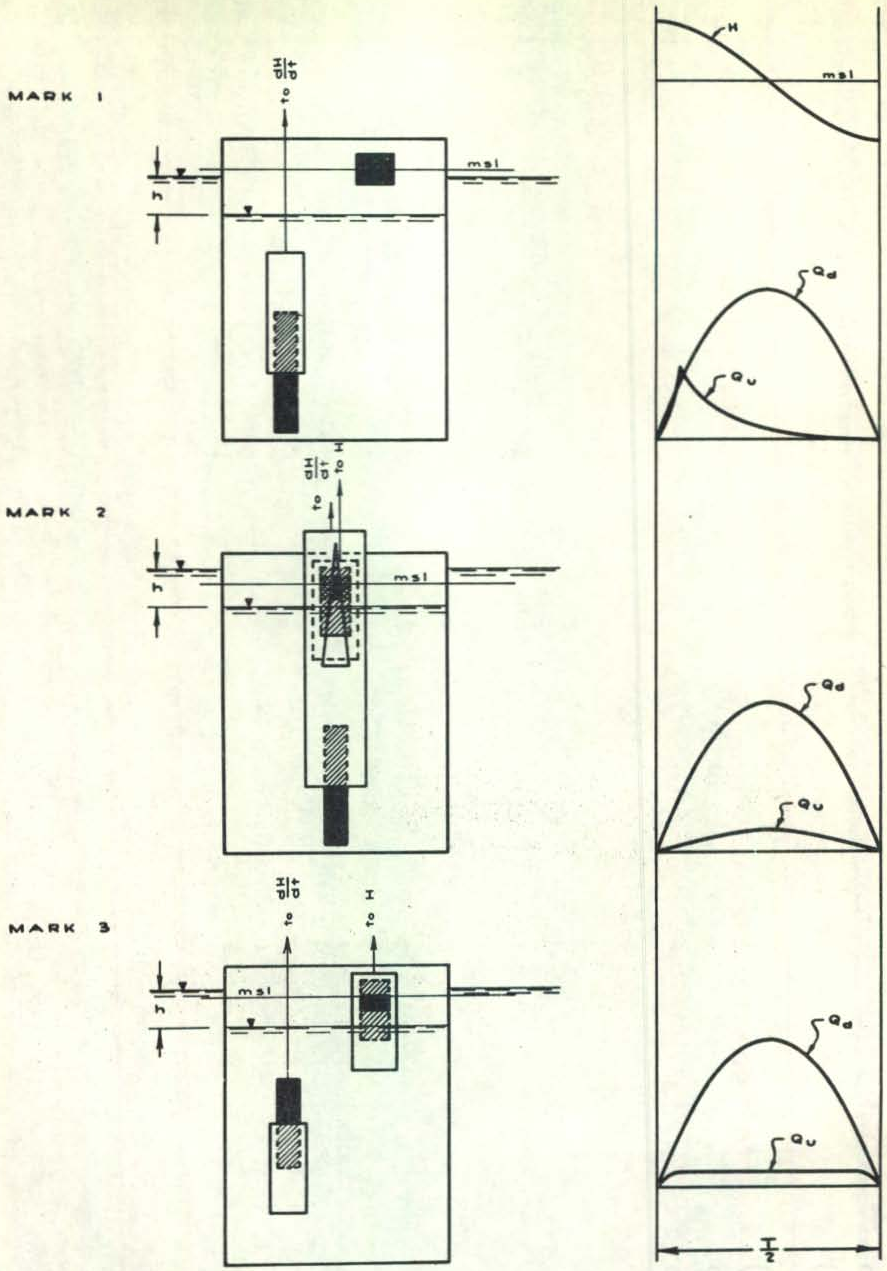

GATE EBB-STANDPIPES

Figure 16

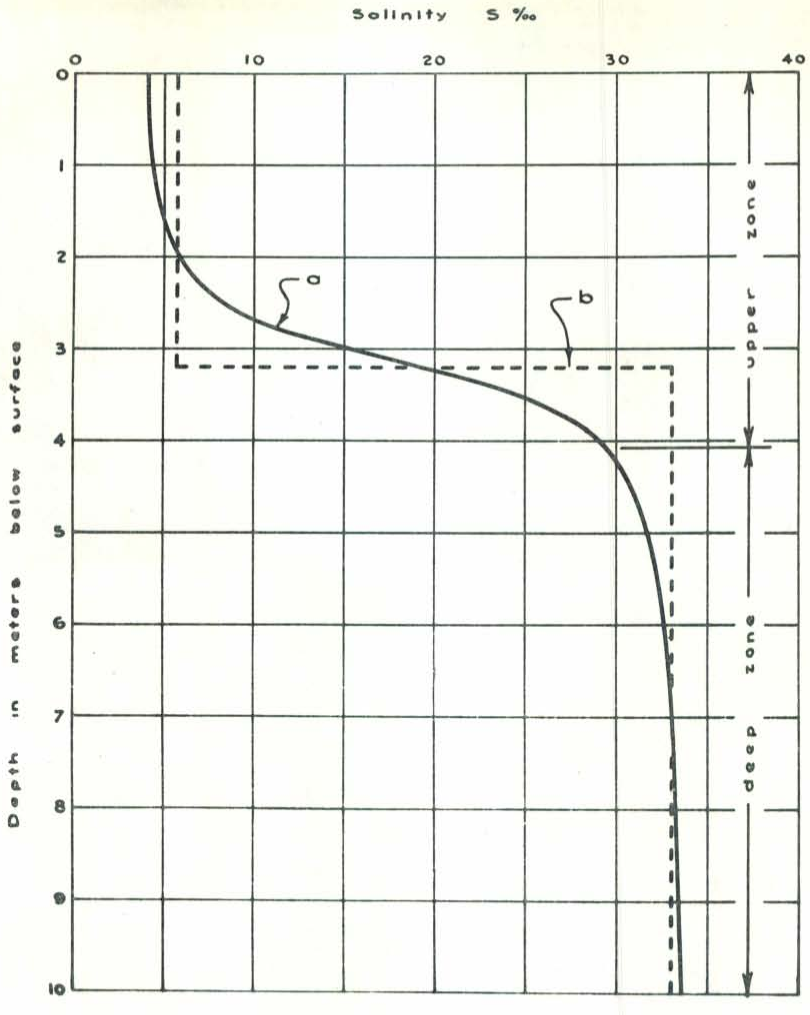

A SALINITY GRADIENT

Figure 17

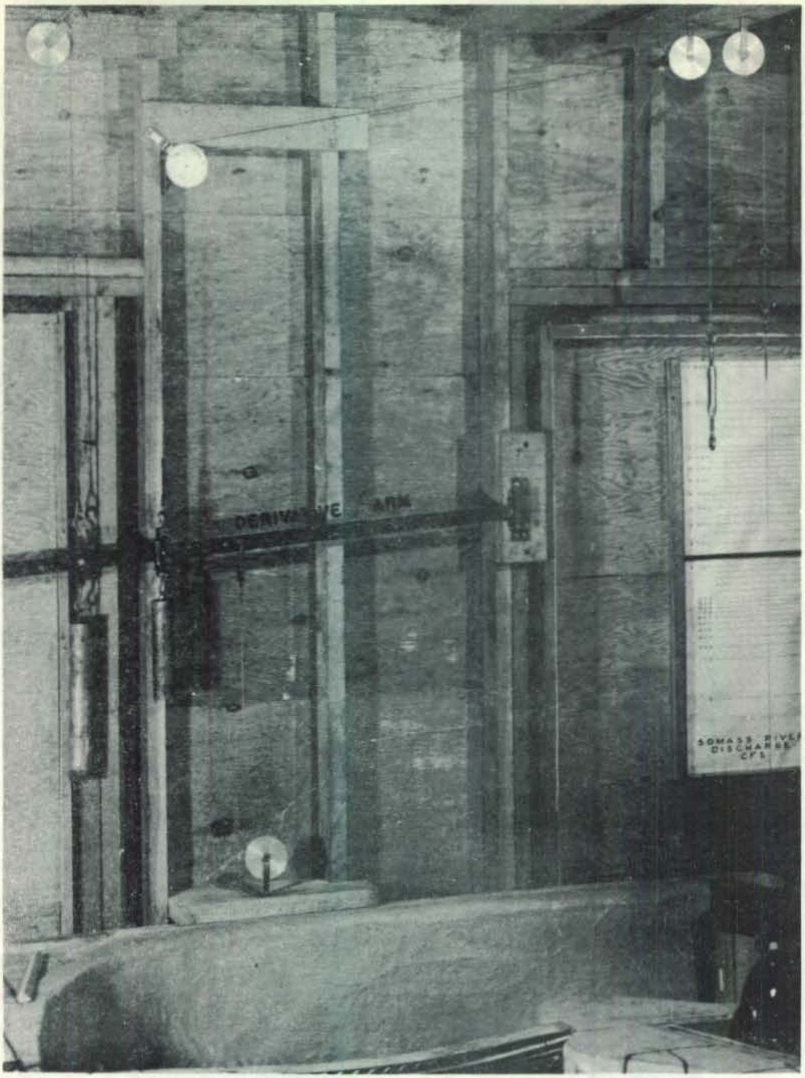

OPERATION OF GATE EBB-STANDPIPE MARK 3

Figure 18

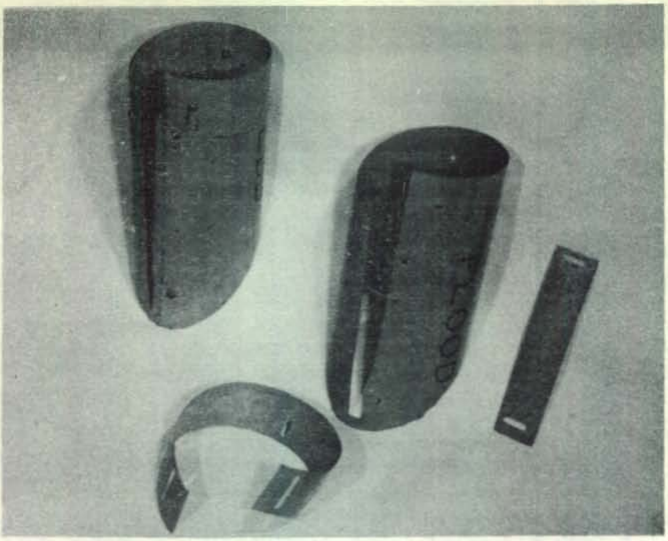

SILL EBB-STANDPIPE

(ASSEMBLED AND DISMANTLED)

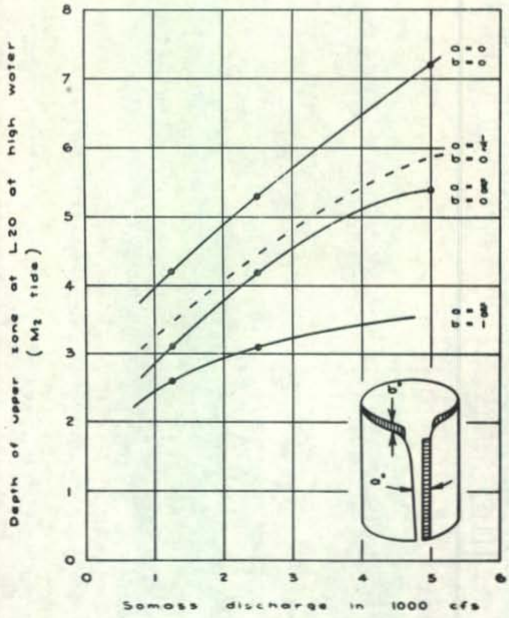

CALIBRATION OF SILL EBB-STANDPIPE

Figure 19